ESTIMATION OF THE CATALYST PELLET ACTIVITY DISTRIBUTION FROM EXPERIMENTAL KINETIC DATA

Alena BRUNOVSKÁ[a], Bibiana REMIAROVÁ[a] and Carlo LEBRUN[b]

[a] *Department of Organic Technology,*
Slovak Institute of Technology, 812 37 Bratislava, Czechoslovakia and
[b] *Dipartimento di Chimica Industriale e Ingegneria Chimica,*
Politecnico di Milano, 201 33 Milano, Italia

In this paper a method of catalyst pellet activity distribution estimation from experimental kinetic data is described. Measurements of outlet concentration from a laboratory continuous stirred single-pellet reactor vs feed rate for ethylene hydrogenation on Pt/alumina pellet are used as kinetic data. To find the best estimate the gradient method is employed and the gradient is computed with the help of the adjoint equation. The estimated activity distribution is compared with the Pt distribution obtained by the scanning electron microscope.

In the preceding papers[1,2] the estimation of catalyst pellet activity distribution from kinetic data has been discussed. The kinetic data have been obtained by measuring outlet concentration of a fixed testing reaction in a stirred tank reactor for various feed rates. The form of the reaction rate expression has been assumed to be known and the system response has been assumed to be sensitive enough to the activity distribution. The last assumption depends not only on the testing reaction choice but also on the experimental conditions. This can be tested by computer simulation of the pellet behaviour. Another point of interest is identification of the volume averaged reaction rate constant and the diffusion coefficient. The value of the volume averaged reaction rate constant can be evaluated from the kinetic region measurements on the crushed pellets. The zero order reaction is one of the few ones which allow to estimate both the mean reaction rate constant and the activity distribution from the same measurements. The same is also true for the diffusion coefficient. For most of the testing reactions to estimate its value along with the activity distribution appears to be an ill-posed problem. (The exception is again the zero order testing reaction.) In any case it is helpful to have some more information about activity, e.g. which part of the pellet is active, or whether the distribution has increasing or decreasing tendency, etc.

In the preceding papers[1,2] the proposed estimation method has been verified on simulated data. In the first paper[1] second order testing reaction has been chosen. In the second paper[2] the zero order reaction has been studied. The aim of this paper
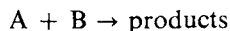
is to estimate catalyst pellet activity distribution from experimental data. The pellet we investigated had a narrow region activity distribution. In this particular case the estimation procedure represents a step in the preparation of catalyst pellets with a desired nonuniform activity ditribution by which the impregnation is controlled. Catalyst pellets of such type are produced in order to increase the effectiveness factor, selectivity or resistance to deactivation.

The following experimental system has been studied: a) γ-alumina catalyst pellet impregnated with Pt, b) hydrogenation of ethylene as the testing reaction (Langmuir–Hinshelwood reaction rate expression).

The reaction rate equation parameters (volume averaged reaction rate constant and adsorption constants) have been estimated from the measurements in the kinetic region on crushed pellets. The ethylene diffusion coefficient and activity distribution have been estimated from the measurements in a laboratory continuous stirred single-pellet reactor. The resulting activity distribution has been compared with the distribution of Pt obtained by the scanning electron microscope combined with energy-dispersive analyser of X-rays.

THEORETICAL

Let us consider a catalyst pellet in a continuous stirred reactor in which the testing reaction

$$A + B \rightarrow products$$

takes place. The dependence of the reactor outlet composition on feed rate under steady state conditions is measured.

The goal of the method we present is to estimate the pellet activity distribution and the diffusion coefficient of component A (D_{eB} has been computed from the relation[3] $D_{eA}/D_{eB} \approx \sqrt{(M_B/M_A)}$ which is a good approximation for both Knudsen and ordinary diffusion) to obtain the best fit of the measured and the computed reactor outlet concentrations. As the objective function

$$F[D_{eA}, \Phi(\varphi)] = \sum_{i=1}^{I} (Y_{Ai} - Y_{Ai,exp})^2 = min \qquad (1)$$

has been used, where Y_{Ai} is the dimensionless reactor outlet concentration corresponding to the activity distribution $\Phi(\varphi)$ and to the diffusion coefficient D_{eA}, $Y_{Ai,exp}$ si the experimental dimensionless concentration and I is the number of measurements.

Two activity distributions $\Phi(\varphi)$ have been considered:

a) a step function (Fig. 1)

$$\Phi(\varphi) = \begin{matrix} 0 & \text{for} & \varphi \notin (\varphi_1, \varphi_2) \\ \gamma = 1/(\varphi_2^{n+1} - \varphi_1^{n+1}) & \text{for} & \varphi \in \langle \varphi_1, \varphi_2 \rangle \end{matrix} \qquad (2)$$

b) a piecewise linear function given by the values $\Phi(\varphi_k)$ in equidistant mesh points dividing the interval $\langle 0, 1 \rangle$. The estimation method has two levels. In the first level using a one-parameter optimization procedure we look for the value of the diffusion coefficient. In the second level we estimate the activity distribution by minimizing the objective function (1) for a given value of the diffusion coefficient.

Mathematical Model

Let us assume perfect gas-to-solid mass transfer, constant temperature in the active layer and constant diffusion coefficients. Then the model dimensionless equations are as follows:

pellet mass balances

$$\nabla^2 Y_A = Th_A^2 R \tag{3}$$

$$\nabla^2 Y_B = \beta Th_A^2 R , \tag{4}$$

boundary conditions

$$\varphi = 0 : dY_A/d\varphi = dY_B/d\varphi = 0 \tag{5}$$

$$\varphi = 1 : Y_A = Y_A(1)$$
$$Y_B = Y_B(1) , \tag{6}$$

reactor mass balances

$$1 - Y_A(1) = Z_{RA}\bar{R} \tag{7}$$

$$1 - Y_B(1) = Z_{RB}\bar{R} , \tag{8}$$

reaction rate equation

$$R = \Phi \frac{\omega^2 Y_A Y_B}{(1 + \varkappa_1 Y_A + \varkappa_2 Y_B)^2} = \Phi \xi(Y_A, Y_B) , \tag{9}$$

and mean reaction rate expression

$$\bar{R} = (n + 1) \int_0^1 R\varphi^n \, d\varphi . \tag{10}$$

From Eqs (3)–(8) and (10) we obtain the boundary conditions

$$\varphi = 1 : dY_A/d\varphi = \frac{Th_A^2}{Z_{RA}(n + 1)} [1 - Y_A(1)] \tag{11}$$

$$dY_B/d\varphi = \frac{Th_A^2 \beta}{Z_{RB}(n + 1)} [1 - Y_B(1)] \tag{12}$$

Eqs $(3)-(8)$ and (11), (12) lead to the following relation between concentrations of components A and B

$$Y_B = Y_B(1) - \beta[Y_A(1) - Y_A]$$ (13)

Using Eq. (13) we can reduce the system of model equations by considering the equations for the component A only. In case of the step function activity distribution we can take into account that the reaction does not take place outside the interval $\langle \varphi_1, \varphi_2 \rangle$, where we obtain the solution of the Eq. (3) in a closed form involving boundary values of Y_A (Eqs (14) and (18) below)

$$\varphi \in \langle 0, \varphi_1) \quad : Y_A = Y_{A1}$$ (14)

$$\varphi = \varphi_1 \quad : dY_A/d\varphi = 0$$ (15)

$$\varphi \in \langle \varphi_1, \varphi_2 \rangle : \nabla^2 Y_A = Th_A^2 R$$ (16)

$$\varphi = \varphi_2 \quad : dY_A/d\varphi = Th_A^2[1 - Y_A(1)]/[Z_{RA}(n + 1) \varphi_2^n]$$ (17)

$$\varphi \in (\varphi_2, 1\rangle \quad : Y_A = Y_A(1) - [Y_A(1) - Y_A(\varphi_2)] \psi_n(\varphi)/\psi_n(\varphi_2).$$ (18)

For both types of activity distributions the system of model equations has been solved numerically. The implicit finite difference scheme has been employed to obtain a system of nonlinear algebraic equations which has been solved by the Newton–Raphson procedure with adjustable step length. As the first iteration the piecewise linear approximation (Fig. 2) satisfying the mean reaction rate expression (10) and the boundary conditions (Eq. (17) or (11)) has been used.
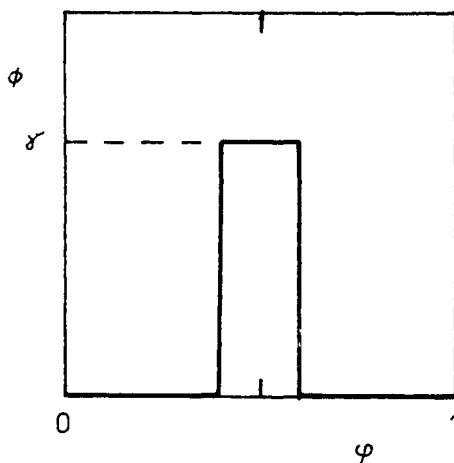

Fig. 1
Step function activity distribution

Optimization Technique

The first level of the optimization procedure consits in estimating the diffusion coefficient (one-parameter optimization). For narrow region activity distribution it is advantageous to employ the step function activity distribution. As the constraints we have the relation for constant amount of active catalyst[1], i.e.

$$(n + 1) \int_0^1 \Phi(\varphi) \, \varphi^n \, d\varphi = 1 \tag{19}$$

and non-negativity of Φ. It is useful to utilize additional information about the active catalyst distribution as an additional constraint. In our case the "visual" method (see Fig. 3) has been used to find the minimum value of φ_1 (the border of the active layer and nonactive pellet center) and the maximum value of φ_2 (the border of the active layer and nonactive pellet shell). This means to estimate the interval $\langle \varphi_{1,\min}, \varphi_{2,\max} \rangle$ for which

$$\Phi(\varphi) = 0 \quad \text{for} \quad \varphi \notin (\varphi_{1,\min}, \varphi_{2,\max})$$

$$\Phi(\varphi) \geqq 0 \quad \text{for} \quad \varphi \in \langle \varphi_{1,\min}, \varphi_{2 \ \max} \rangle \ . \tag{20}$$

For each value of the diffusion coefficient D_{eA} we have to estimate the activity distribution minimizing the objective function (1). For the step function representation,
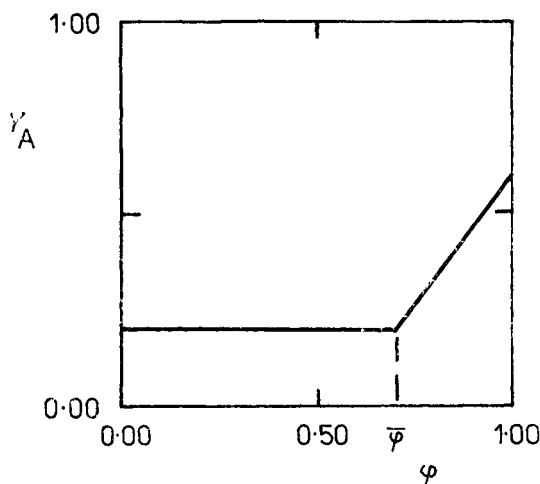

Fig. 2

The choice of first iteration. For step function activity distribution representation the point $\bar{\varphi}$ is from the interval $\langle \varphi_1, \varphi_2 \rangle$
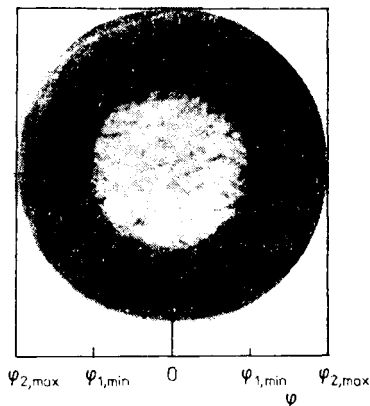
Fig. 3

The cross pellet section

the objective function has two parameters φ_1 and φ_2 which have been estimated by the simplex method[4]. In case of the piecewise linear representation, the objective function has K parameters $\Phi(\varphi_1)$, $\Phi(\varphi_2)$, ..., $\Phi(\varphi_K)$. To find the minimum of the function (1) a gradient type method has been employed. The gradient is the vector with the components

$$\frac{\partial F}{\partial \Phi(\varphi_k)} = \sum_{i=1}^{I} \left\{ -(n+1) \, Th_A^2 \int_{\varphi - \Delta\varphi/2}^{\varphi + \Delta\varphi/2} \varphi^n (p_{Ai} + \beta p_{Bi}) \, \xi_i \, \mathrm{d}\varphi \right\} \quad k = 1, 2, ..., K \qquad (21)$$

and p_A, p_B are the adjoint variables, which solve the adjoint equations

$$\nabla^2 p_A = (p_A + \beta p_B) \, Th_A^2 \Phi \, \frac{\partial \xi}{\partial Y_A} \qquad (22)$$

$$\nabla^2 p_B = (p_A + \beta p_B) \, Th_A^2 \Phi \, \frac{\partial \xi}{\partial Y_B} \qquad (23)$$

with boundary conditions

$$\varphi = 0 : \mathrm{d}p_A/\mathrm{d}\varphi = \mathrm{d}p_B/\mathrm{d}\varphi = 0 \qquad (24)$$

$$\varphi = 1 : \mathrm{d}p_A/\mathrm{d}\varphi = [Y_A(1) - Y_{As} - p_A(1) \, Th_A^2/Z_{RA}]/(n+1) \qquad (25)$$

$$\mathrm{d}p_B/\mathrm{d}\varphi = [-p_B(1) \, \beta Th_A^2/Z_{RB}]/(n+1) . \qquad (26)$$

The derivation of the gradient components and the system of the adjoint equations is similar as for the n-th order reaction (see Appendix of the preceding paper[1]).

Because of the constraint (19) and the non-negativity of $\Phi(\varphi_k)$ the projected gradient method has been used. The $(m+1)$-th iteration has been computed from the m-th one by the scheme

$$\Phi(\varphi_k) = \frac{\Phi(\varphi_k)^m - \lambda^m y_k}{(n+1) \int_0^1 (\Phi(\varphi_k)^m - \lambda^m y_k) \, \varphi^n \, \mathrm{d}\varphi} , \qquad (27)$$

where

$$y_k = \begin{pmatrix} \partial F/\partial \Phi(\varphi_k) & \text{for} & \Phi(\varphi_k) > \varepsilon & \text{or for} & \Phi(\varphi_k) \leq \varepsilon & \text{and} & \partial F/\partial \Phi(\varphi_k) \leq 0 \\ 0 & \text{for} & \Phi(\varphi_k) \leq \varepsilon & \text{and} & \partial F/\partial \Phi(\varphi_k) > 0 \end{pmatrix} \qquad (28)$$

and the step length λ^m has been determined by a one-parameter optimization procedure in the gradient direction (the method of steepest descent). As the first approximation of the activity distribution the parabolic function has been chosen (see Fig. 6).

EXPERIMENTAL

Catalyst Preparation

Cylindrical tablets (diameter 1·45 cm, length 1·5 cm) obtained by compression of Al_2O_3 powder have been calcinated at 500°C for 6 h. Physical properties of the support (specific surface area 207·5 m^2/g, pore volume 0·487 cm^3/g, average pore diameter 4·70 nm) have been determinated by the nitrogen sorption method.

The plane faces of pellets have been covered with stearic acid before the impregnation to avoid axial diffusion of active species. The impregnating solution has been prepared by adding 0·05M solution of hexachloroplatinic acid and 0·1M citric acid solution in the volumetric ratio 1 : 1. The experimental procedure[5] involved placing of the support pellets in contact with impregnating solution for 23 h at 25°C. Removed pellets have been washed with distilled water, dried in air at 120°C for 6 h and reduced in flowing hydrogen at 500°C for 2 h. Residual impregnating solution combined with wash water has been analyzed for platinum spectrophotometrically. The platinum content in the catalyst pellet was approx. 3 wt. %.

The radial distribution of platinum through the catalyst pellet was measured by electron microanalysis using a scanning electron microscope equipped with an analyzer of the X-ray dispersion EDAX (see Fig. 5).

Testing Reaction

To estimate the activity distribution hydrogenation of ethylene has been selected as a testing reaction.

$$CH_2{=}CH_2 \; + \; H_2 \quad \xrightarrow{\;Pt/Al_2O_3\;} \quad CH_3{-}CH_3\,, \quad \Delta H = -136{\cdot}9 \text{ kJ/mol}\,.$$
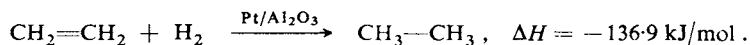
The kinetic model of this reaction has been investigated and described in literature[6,7]. In the recent paper[7] the proposed kinetic model is described by several reaction sequences. From the practical point of view we prefer the more simple one, which is described by one rate equation

$$r = k_w K_A K_B P_A P_B / (1 + K_A P_A + K_B P_B)^2 \qquad (29)$$

and which provides quite a good description for our experimental kinetic data in the investigated interval. The temperature dependence of the rate constant k_w and the adsorption constants K_A, K_B have been considered by the Arrhenius equation, i.e.

$$
\begin{aligned}
k_w &= k_{wo} \exp\left[-E/(RT)\right] \\
K_A &= K_{Ao} \exp\left[-Q_A/(RT)\right] \\
K_B &= K_{Bo} \exp\left[-Q_B/(RT)\right]\,.
\end{aligned}
\qquad (30)
$$

Rotating Basket Reactor Measurements

The kinetic measurements of the testing reaction have been carried out in an isothermal gradientless rotating basket reactor. The catalyst for kinetics measurements has been prepapred by the following procedure: the catalyst pellet obtained in the way mentioned above has been transformed to fine powder and the cylindrical tablet has been repressed from it. It means that the repressed pellet contained the same amount of platinum as the original one but uniformly distributed. The new pellet has been crushed to a grain size below 3 mm and used for kinetic measure-

ments in the rotating basket reactor. The reaction kinetics has been measured at six temperatures in the range from 40° to 90°C, at each temperature for three different feed stream compositions. The ethylene concentration in the outflowing stream has been analyzed by a gas chromatograph. The experimental conditions are given in Table I. The values of the reaction rate equation parameters estimated from the rotating basket reactor measurements are in Table II.

TABLE I

Experimental rotating basket reactor measurements conditions

Temperature, K	313—363
Pressure, Pa	$1.25 . 10^5$
Concentration ratio of ethylene and hydrogene	0.3; 0.5; 1.0
Inlet ethylene concentration, mol m^{-3}	12.5—25.3
Mass of catalyst, g	0.124
Catalyst particle diameter, mm	1.5—2.5
Volumetric flow rate, 10^6 m^3 s^{-1}	0.67—6.67

TABLE II

Reaction rate equation parameters

k_{wo}	$0.293 . 10^2$ mol kg_{cat}^{-1} s^{-1}
K_{1o}	$0.213 . 10^{-4}$ Pa^{-1}
K_{2o}	$0.759 . 10^{-6}$ Pa^{-1}
E	$-0.200 . 10^5$ J mol^{-1}
Q_A	$0.266 . 10^5$ J mol^{-1}
Q_B	$-0.440 . 10^4$ J mol^{-1}

TABLE III

Experimental single-pellet reactor measurements conditions

Pressure, Pa	$1.25 . 10^5$
Concentration ratio of ethylene and hydrogene	0.3; 0.5; 1.0
Inlet ethylene concentration, mol m^{-3}	12.71; 16.91; 25.36
Mass of catalyst, g	2.272
Catalyst particle diameter, mm	14.5
Volumetric flow rate, 10^6 m^3 s^{-1}	0.67—5.33

Single-pellet Reactor Measurements

The catalyst pellet with nonuniform platinum distribution has been placed in the continuous stirred tank reactor in such a way that the reacting gas has been in contact with the lateral surface of the cylinder only. The gaseous phase of volume 100 ml has been extensively mixed in order to enable us to assume uniform concentration through the reactor and to neglect external diffusion. The temperature in the jacket of the reactor has been regulated to 30°C. The temperatures of the reactor gas phase and in the several points of the pellet (external surface, active layer and
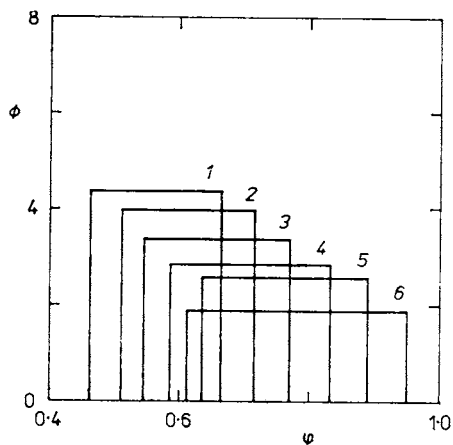
FIG. 4

Optimal step function activity distribution for several values of $D_{eA} \cdot 10^5$ (m^2 s^{-1}): *1* 1·5, *2* 1·25, *3* 1·0, *4* 0·75, *5* 0·5, *6* 0·25
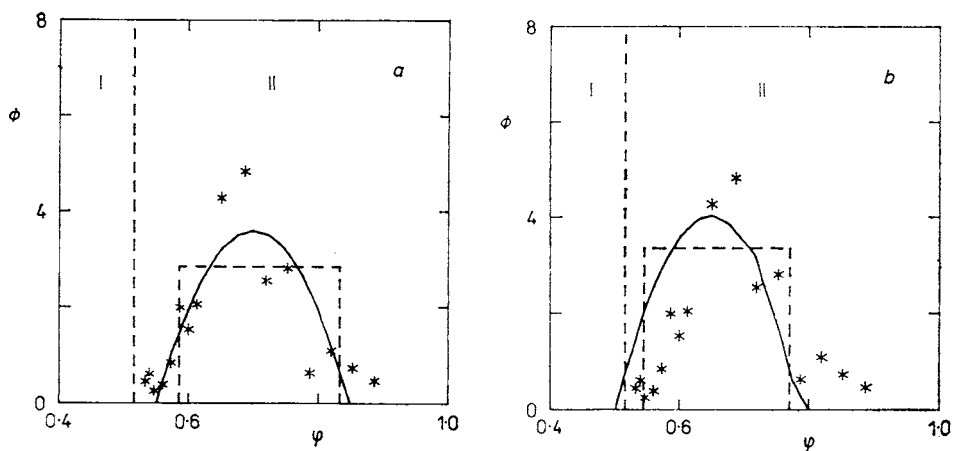
FIG. 5

Resulting activity distribution for step function (-----) and piecewise linear function (———) representation with normalized amount of Pt (*). *a* I white pellet, II dark pellet, $D_e = 0.75$. 10^{-5} m^2 s^{-1}; *b* I white pellet, II dark pellet, $D_e = 1.0$. 10^{-5} m^2 s^{-1}

pellet center) have been measured by iron–copper thermocouples. The outlet ethylene concentration has been analyzed by gas chromatograph. The experimental conditions are in Table III.

The kinetic equation parameters for each experiment have been computed from Eq. (*30*) for measured active layer temperature.

RESULTS AND DISCUSSION

The optimal step function activity distribution for six values of the diffusion coefficient D_{eA} are shown in Fig. 4. With the increase of D_{eA} the optimal activity distribution is moving towards the pellet center. The lowest values of the objective function (*1*) have been achieved in the interval $D_{eA} \in \langle 0.75 \cdot 10^{-5}, 1.0 \cdot 10^{-5} \rangle$ m^2/s, but the differences between the values of the objective function for all illustrated examples are not significant. This is why we used another criterion for finding D_{eA}, viz. comparison of the computed step function activity distribution with the detailed pellet photograph. The step function must coincide with the dark region of the pellet.

The estimated non-parametric activity distributions for the two values of D_{eA} are in Fig. 5. In this figure the resulting activity distributions are compared with the normalized Pt distribution (ratio of Pt amount and total Pt amount in the pellet) from the scanning electron microscope. The best coincidence is for $D_{eA} = 0.75 \cdot 10^{-5}$ m^2/s, which provides also the lowest value of the objective function.
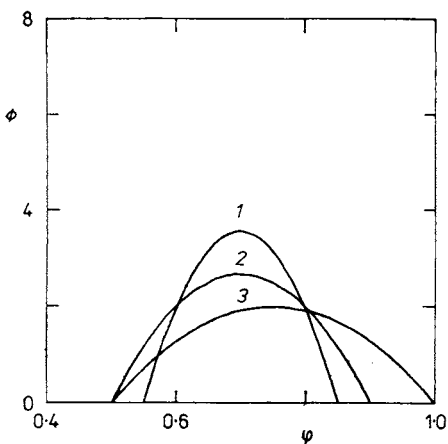

FIG. 6

The choice of first iteration for the gradient method ($D_{eA} = 0.75 \cdot 10^{-5}$ m^2 s^{-1}); *F: 1* 0·0139, 2 0·0184, 3 0·3740
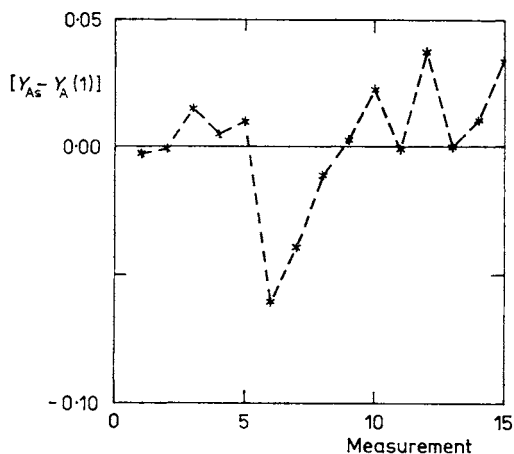
FIG. 7

The difference between experimental and theoretical reactor outlet concentrations ($D_{eA} = 0.75 \cdot 10^{-5}$ m^2 s^{-1})

In Fig. 6 the strategy for finding the first iteration for the gradient method (by comparison of the objective function for several parabolic activity distributions) is illustrated.

The difference of the computed and the mesured reactor outlet concentrations is in Fig. 7.

From the illustrated example it is evident that the reactor outlet concentration is sensitive to the pellet activity distribution, i.e. that the choice of the testing reaction and experimental conditions appears to be suitable. For this particular case (narrow region activity distribution) also the step function activity representation provides quite a good coincidence between the experimental and the theoretical data. The results obtained indicate that the proposed gradient type estimation method works well for experimental data.

LIST OF SYMBOLS

a	characteristic dimension of catalyst pellet, m
C	concentration, mol m^{-3}
D_e	diffusivity coefficient, m^2 s^{-1}
E	activation energy, J mol^{-1}
F	objective function, mol^3 m^{-6}
k_w	reaction rate constant, mol kg^{-1} s^{-1}
K	adsorption constant, Pa^{-1}
n	integer characteristic of pellet geometry
p	adjoint variable
P	partial pressure, Pa
Q	adsorption heat, J mol^{-1}
r	reaction rate, mol kg^{-1} s^{-1}
R	dimensionless reaction rate, $R = r/r_0$
t	time, s
T	temperature, K
Th	Thiele modulus, $Th = a \sqrt{[r_0 \varrho/(D_{eA} C_{Ao})]}$
V	volume of the gas phase of the reactor, m^3
V_f	volumeric flow rate, m^3 s^{-1}
W	catalyst mass, kg
Y	dimensionless concentration, $Y = C/C_0$
Z_{RA}	dimensionless parameter, $Z_{RA} = r_0 W/(V_f C_{Ao})$
Z_{RB}	dimensionless parameter, $Z_{RB} = r_0 W/(V_f C_{Bo})$
β	dimensionless parameter, $\beta = D_{eA} C_{Ao}/(D_{eB} C_{Bo})$
γ	activity (step function activity distribution, Eq. (2))
ε	accuracy
$\varkappa_1$	$= K_A C_{Ao}$
$\varkappa_2$	$= K_B C_{Bo}$
ζ	concentration term in dimensionless reaction rate (Eq. (9))
ϱ	pellet density, kg m^{-3}

τ	dimensionless time, $\tau = tD_A/a^2$
φ	dimensionless position, $\varphi = r/a$
Φ	activity
ψ	function of pellet geometry (for $n = 1$, $\psi_n = \ln \varphi$)
ω	rate equation parameter, $\omega = 1 + \varkappa_1 + \varkappa_2$

Subscripts

A	ethylene
B	hydrogen
o	feed stream conditions
1, 2	for φ_1, φ_2

REFERENCES

1. Brunovská A., Horák J.: Collect. Czech. Chem. Commun. *52*, 2412 (1987).
2. Brunovská A., Horák J.: Collect. Czech. Chem. Commun. *52*, 2426 (1987).
3. Satterfield Ch. N., Sherwood T. K.: *The Role of Diffusion in Catalysis.* Addison–Wesley, Reading Mass. 1963.
4. Beveridge G. S. G., Schechter R. S.: *Optimization. Theory and Practice.* McGraw–Hill, New York 1970.
5. Shyr Y., Ernst W. R.: J. Catal. *63*, 425 (1980).
6. Rogers G. B., Lih M. M., Hougen O. A.: AIChE J. *12*, 369 (1966).
7. Prairie M. R., Bailey J. E.: Chem. Eng. Sci. *42*, 2085 (1987).

Translated by the author (A.B.).